THz Backward-Wave Oscillators for Plasma Diagnostic in Nuclear Fusion

Claudio Paoloni, *Senior Member, IEEE*, Diana Gamzina, Logan Himes, Branko Popovic, Robert Barchfeld, Lingna Yue, Yuan Zheng, Xiaopin Tang, Ye Tang, Pan Pan, Hanyan Li, Rosa Letizia, *Member, IEEE*, Mauro Mineo, Jinjun Feng, *Senior Member, IEEE*, and Neville C. Luhmann, Jr., *Fellow, IEEE*

***Abstract*— Understanding of the anomalous transport attributed to short-scale length microturbulence through collective scattering diagnostics is key to the development of nuclear fusion energy. Signals in the subterahertz (THz) range (0.1–0.8 THz) with adequate power are required to map wider wavenumber regions. The progress of a joint international effort devoted to the design and realization of novel backward-wave oscillators at 0.346 THz and above with output power in the 1 W range is reported herein. The novel sources possess desirable characteristics to replace the bulky, high maintenance, optically pumped far-infrared lasers so far utilized in this plasma collective scattering diagnostic. The formidable fabrication challenges are described. The future availability of the THz source here reported will have a significant impact in the field of THz applications both for scientific and industrial applications, to provide the output power at THz so far not available.**

***Index Terms*— Backward-wave oscillator (BWO), double-corrugated waveguide (DCW), double-staggered grating (DSG), plasma diagnostic, terahertz (THz).**

I. Introduction

TERAHERTZ (THz) vacuum electron devices are gaining significant consideration when the generation of relatively high power in the frequency range below 1 THz is needed [1]–[9]. In particular, the backward-wave oscillator (BWO) is an effective solution to produce relatively high power and stable monochromatic THz signals. BWOs can be electronically tuned over a wide frequency range around the operating frequency and have high stability in frequency (up to 10^{-7} to 10^{-8} by phase locking). However, the only available BWOs are based on old technologies. No compact, affordable, and long-life THz BWOs is currently available.

Recently, the introduction of new high aspect-ratio fabrication processes derived from the MEMS technologies as the lithography, electroplating, and molding (LIGA) [5], [7] and advanced mechanical microfabrication as nano-CNC milling [10] provides an accuracy at the submicrometer level, which satisfies the demanding specifications of interaction structures or slow-wave structures (SWSs) to support the THz operation frequencies. Furthermore, the progress on simulation tools based on accurate 3-D electromagnetic and particle-in-cell (PIC) solvers permits now a reliable prediction of the THz vacuum source performance, to ease the fabrication phase. The development of innovative cathode materials [10] is leading to a novel generation of electron guns, with high current density and long lifetime, fundamental for the overall device mean time between failures and high-frequency stability. Nevertheless, the main challenges are to achieve a surface roughness below the skin depth (66 nm at 1 THz) for minimizing the ohmic losses and the assembly and alignment of the beam with tolerance in the order of tens of micrometers.

Nuclear fusion is one of the fields, where the availability of THz BWOs will have a relevant impact on improving the understanding of a critical phenomenon as the anomalous transport of the plasma. It still remains a fundamental area of investigation, which is essential for the development of fusion energy. The measurement technique is based on the collective Thomson scattering at THz frequency [12]–[15]. The plasma is illuminated by a THz beam that is scattered by the charged particles. The scattered beams due to the electron density fluctuations are detected by a receiver array and thereby map out the location, wavenumber spectrum, and strength of the turbulence.

In the recent upgrade of the high-k scattering system at NSTX experiment at Princeton, the wavenumber k_θ coverages, and it has been increased to target electron temperature gradient modes by increasing the probe frequency from 0.280 to 0.693 THz. The availability of solid-state sources is limited to about 0.3 THz and 30 mW, while about 100 mW are needed at 0.693 THz to excite a detectable scattering.

Manuscript received November 1, 2015; revised February 5, 2016; accepted March 9, 2016. This work was supported in part by the National Science Foundation through the Major Research Instrumentation Program under Grant CHE-1429258, in part by the U.S. Department of Energy, National Spherical Torus Experiment under Grant DE-FG02-99ER54518, in part by the U.S. Department of Defense under Grant M67854-06-1-5118, in part by the Defense Advanced Research Projects Agency, Defense Sciences Office, under Grant G8U543366, in part by the U.K. Engineering and Physical Sciences Research Council under Grant EP/L026597/1, and in part by the ATK's Alliance Partnership Program, which was provided via the use of their MAGIC software.

C. Paoloni and R. Letizia are with Lancaster University, Lancaster LA1 4YW, U.K. (e-mail: c.paoloni@lancaster.ac.uk; r.letizia@lancaster.ac.uk).

D. Gamzina, L. Himes, B. Popovic, R. Barchfeld, and N. C. Luhmann, Jr., are with the Department of Electrical and Computer Engineering, University of California at Davis, Davis, CA 95616 USA (e-mail: dgamzina@ucdavis.edu; lghimes@ucdavis.edu; bkpopovic@ucdavis.edu; rbarchfeld@ucdavis.edu; ncluhmann@ucdavis.edu).

L. Yue, Y. Zheng, and X. Tang are with the University of Electronic Science and Technology of China, Chengdu 610051, China (e-mail: lnyue@uestc.edu.cn; zyzheng@ucdavis.edu; xiaopintang@gmail.com).

Y. Tang, P. Pan, H. Li, and J. Feng are with the Vacuum Electronics National Laboratory, Beijing Vacuum Electronic Research Institute, Beijing 100016, China (e-mail: tangye1983@163.com; p-pan@hotmail.com; fengjinjun@tsinghua.org.cn).

M. Mineo is with e2v Technologies Ltd., Chelmsford CM1 2QU, U.K. (e-mail: m.mineo@e2v.com). mauro.mineo@e2v.com

Color versions of one or more of the figures in this paper are available online at http://ieeexplore.ieee.org.

Digital Object Identifier 10.1109/TPS.2016.2541119

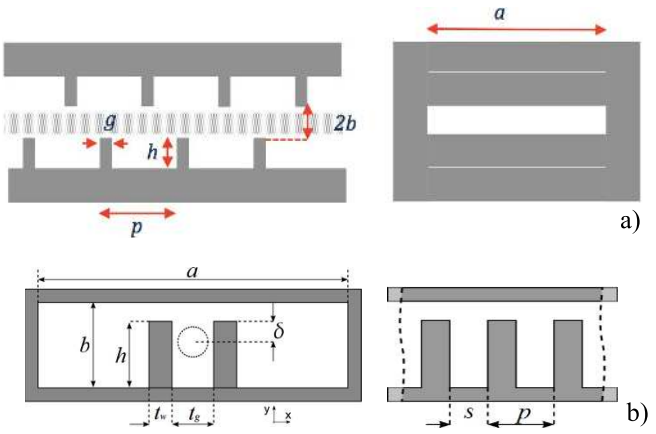

Fig. 1. SWS for 0.346-THz operation. (a) DSG. (b) DCW. The gray area in (a) and the dashed circle in (b) represent the sheet and cylindrical beam for the DSG and the DCW, respectively.

Presently, the only THz source to deliver ∼100 mW at 0.693 THz needed to provide the minimum scattered signal level to be detected by the receiver array is a bulky optically pumped far infrared. A second high-frequency source is needed to provide local oscillator (LO) power for the receiver array. The use of a second laser is not feasible. It has been chosen to use an array based on sensitive room temperature subharmonic mixers working roughly at half of the illumination source frequency, namely, 0.346 THz. It is required 3 to 5 mW of LO power per mixer.

This paper describes an international joint effort of three leading institutions in China, the U.K., and the U.S. to design and construct a novel family of BWOs, operating at the frequency of 0.346 THz, to satisfy the quest for LO power for the matrix array for the NSTX-U plasma diagnostic and other future plasma diagnostic systems [16]. The design target is to achieve an output power in the range of hundreds of milliwatt by lightweight, compact, affordable, low-operating cost BWOs to enable a wide matrix of receivers.

This paper is organized as follows. The properties of two different SWSs suitable for THz BWO fabrication are reported in Section II. Section III describes the design aspects and the cold parameters. Section IV details the hot simulations and performance of the two BWOs. Challenges involved with microfabrication technologies of the proposed BWOs are discussed in Section V. Section VI reports on the gun and the window.

II. Terahertz Slow-Wave Structures

At microwave frequencies, helices are the most common SWSs, but as the frequency increases toward the millimeter-wave range, their dimensions are too small for fabrication, and new geometries must be adopted. The simple structure of the rectangular corrugated waveguide inspired different structures that can be realized by the available fabrication processes with the dimensions to support THz frequencies.

In particular, the double-staggered grating (DSG) [17] [Fig. 1(a)] and the double-corrugated waveguide (DCW) [18] [Fig. 1(b)] are the two SWSs that have been successfully proposed for operation at THz frequencies and overcome the fabrication issues of the conventional structures.

The DSG is conceived to support an elliptical sheet electron beam. The advantage of the sheet electron beam is the large cross section that permits to deliver a high beam current using a relatively beam current density. The sheet beam requires a careful design of the magnetic focusing system, but it is very promising to realize high-power vacuum electron devices by using low cathode loading guns.

The DCW is conceived to support a cylindrical electron beam. The DCW is of easy fabrication and assembly. The advantage of a cylindrical electron beam is that it is generated by the well-established Pierce gun technology and focused by the use of a conventional magnetic focusing system.

Both the SWSs are very promising to realize THz BWOs with a wide range of characteristics in terms of fabrication, output power, and cost.

III. BWO Design

The approach of using two different SWSs, the DSG and the DCW, to design a family of THz BWO is a breakthrough for tailored power generation at THz frequencies. Two BWOs based on the DSG and the DCW will be the first two devices for a new family of THz sources to cover a wide range of applications.

The main design targets are given in the following:

1) low cost;
2) easy assembly for high yield;
3) compact dimensions (200–300 cm^3);
4) wide range of performance to potentially cover the sub-THz spectrum (0.1–1 THz);
5) tunable (at least 5%);
6) low beam voltage and compact power supply.

A 0.346-THz operating frequency is considered in the following for application in the plasma diagnostic in nuclear fusion, as described in Section I. The first design parameter defined was the beam voltage that determines the length of the period of the SWSs. A low beam voltage in the range of 12–18 kV favors to use of a compact and low-cost power supply. The resulting period was estimated to be in the range of the fabrication process.

Due to the different structures, different beam voltages were adopted. The DSG was designed to operate with 17-kV beam voltage, while the DCW was to support about 13 kV. The dimensions of the two SWSs are shown in Table I. It is notable that a period shorter than 200 μm is required. In Fig. 2, the dispersion curve of the DCW with superimposed beam line at 12.8 kV is shown. The interaction impedance is typically low in the backward-wave mode.

1) Couplers: A detailed study based on 3-D electromagnetic simulation [18] on the coupler to transform the mode in the SWS in the TE_{10} at the flange at the output port was carried out to maximize power transfer. The conductivity of copper considered in simulation is $\sigma_{cu} = 3.9 \times 10^7$ S/m [7]. The coupler is a three-port network; one port is connected to the SWS, a second port is the beam tunnel to connect the gun, and the third port is the output port connected to the flange.

AQ:5

TABLE I

DSG		DCW	
Parameter	µm	Parameter	µm
a	483	a	1500
b	45	b	200
h	170	h	140
p	185	p	140
g	44	s	80
		t_g	120
		t_w	60

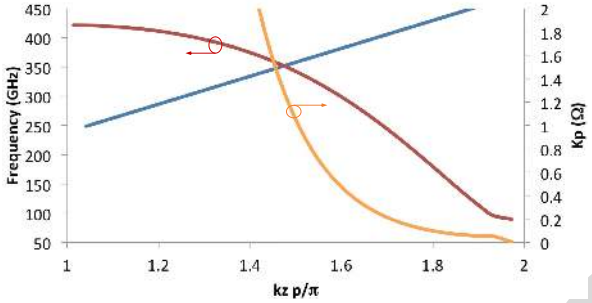

Fig. 2. DCW dispersion curve (brown curve), interaction impedance (orange curve), and beam line at 12.8 kV (blue line).

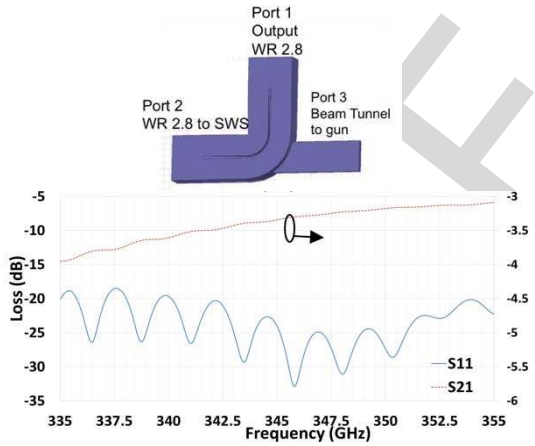

Fig. 3. DSG coupler S-parameters.

The coupler for the DSG is particularly challenging due to the wide beam tunnel needed for the sheet beam. Having a low cutoff frequency in the same range of the SWS, a ridge is added to the bend (Fig. 3) to perturb the matching between the SWS and the beam tunnel. The resulting S_{11} is better than -25 dB over a wide frequency range around 0.346 THz.

A study of the coupler for the DCW was performed by considering a back-to-back structure. First, a simple structure including a tapered transition between a waveguide with the same cross section of the DWG and the flanges is designed, as shown in Fig. 4(a), to evaluate the effect of the

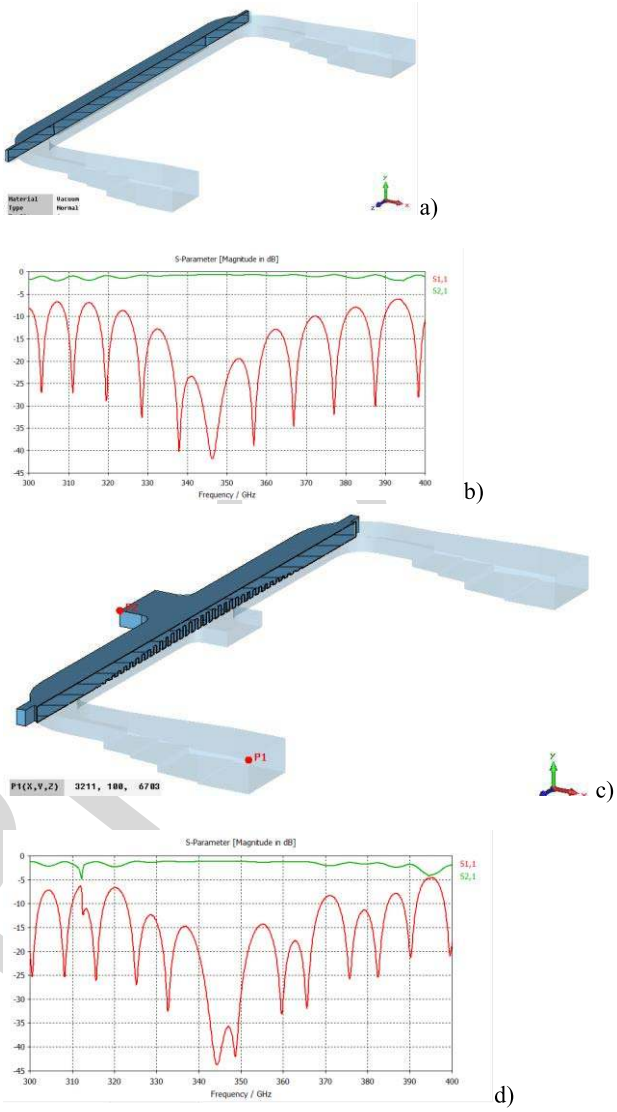

Fig. 4. DCW coupler. (a) Waveguide without DCW. (b) S-parameter structure. (c) Waveguide with DCW. (d) S-parameters.

AQ:6

waveguide tapering. Fig. 4(b) shows the obtained S_{11} better than -25 dB in the operation range. Next, a second structure with similar topology, including three sections of pillars (two tapered sections and one short section with a nominal height), is designed for the best matching, as shown in Fig. 4(c). Results show that S_{11} in this case is better than -35 dB in the region around the operating frequency [Fig. 4(d)].

Both the couplers' performance ensures the efficient propagation of the RF signal from the interaction structure to the flanges.

IV. Large Signal Simulations

The design of the two BWOs is based on the definition of the critical length for oscillations to set a proper number of periods within the SWS. Results from this optimization process are shown in Table II.

Next, the 3-D PIC simulations performed to evaluate the electrical behavior of the BWOs. The DSG BWO supports an

TABLE II

BWO specifications	DSG	DCW
Beam Voltage	17.1 kV	12.8 kV
Beam current	14 mA	10 mA
Beam channel	483 x 90 μm	120 μm
Beam Aspect Ratio	5.4 : 1	Round
Beam Current Density	160 A/cm^2	127 A/cm^2
Magnetic field	0.35 T	0.5 T
No. Periods	65	116
Total length	~ 15 mm	~ 20 mm

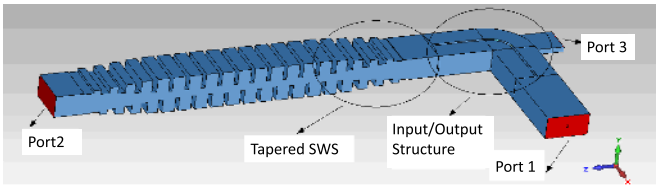

Fig. 5. PIC simulation setup for the DSG BWO.

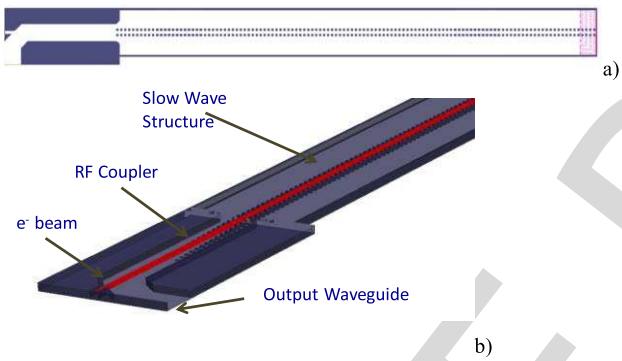

Fig. 6. PIC simulation setup for the DCW PIC simulations. (a) Top view. (b) Coupler detail.

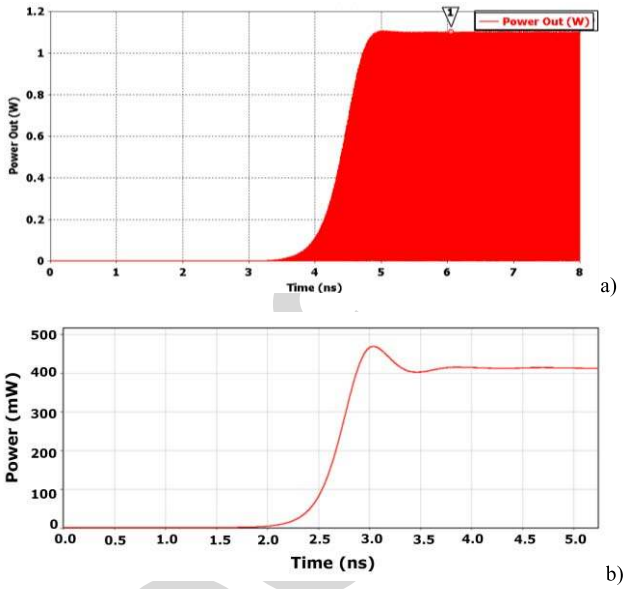

Fig. 7. Average output power for (a) DSG and (b) DCW BWOs.

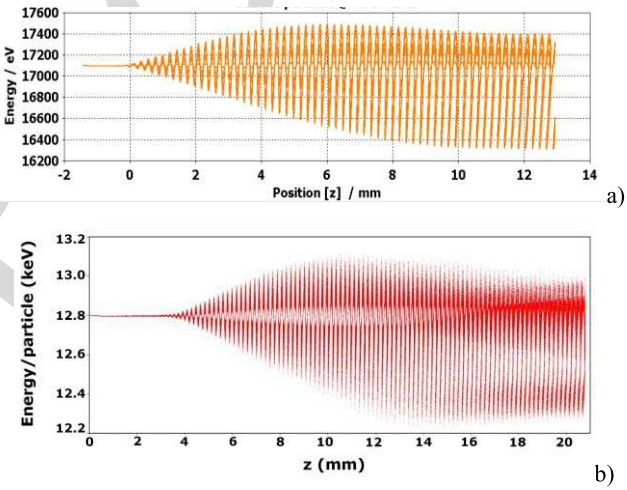

Fig. 8. Electron energy. (a) DSG BWO. (b) DCW BWO.

elliptical electron beam with the cross section of $400 \times 50\ \mu m^2$ and the current of 14 mA (the aspect ratio of 5.4:1). The DWC BWO supports a cylindrical electron beam of 50-μm radius and 10-mA current. Due to the different beam parameters used, the overall device performance is different for the two BWOs and should be evaluated in the context of the different technological challenges required and the different application needs. The DSG BWO is modeled by CST Particle Studio [19] (simulation setup in Fig. 5) and the DCW BWO is modeled by MAGIC3D [20] (simulation setup in Fig. 6).

The results of output power for the two devices are shown in Fig. 7. The DSG BWO [Fig. 7(a)] provides about 1 W and the DCW BWO about 0.4 W [Fig. 7(b)]. The electron energy distribution along the longitudinal direction for both the BWOs is shown in Fig. 8. The spectral response at the output port of the DCW BWO is shown in Fig. 9, showing the highly monochromatic generation of signal at the frequency of interest.

In order to demonstrate the tunability of the BWO designs, the tuning range for the DSG and the DCW is shown in Fig. 10(a) and (b), respectively. It can be noted that a variation of beam voltage in the range of 15.8–17.8 kV permits a variation in frequency of 12 GHz for the DSG and that the same relative change in the nominal beam voltage allows a tuning of 14 GHz for the DCW.

The BWO performances so far presented are at the state of the art. The high power level and tuning features, not achievable by any other technology today, represent a breakthrough in the field.

V. BWO Microfabrication

The main challenge in the THz frequency range is the fabrication of SWSs with the expected electromagnetic behavior while establishing a reliable and repeatable process. For the DSG circuit, vane height is the most sensitive dimension which determines the bandwidth of the device. The period of the structure affects the central operating frequency, whereas the width of the DSG controls the dispersion curve. The DCW structure is more sensitive to the h and p values driving the

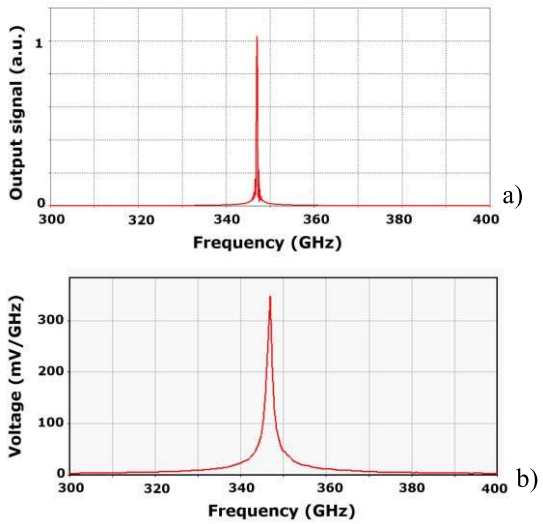

Fig. 9. Spectrum of (a) DSG and (b) DCW BWOs.

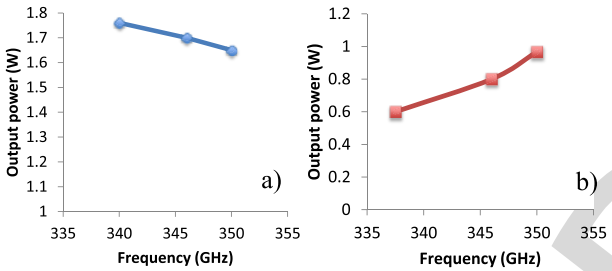

Fig. 10. Instantaneous power and tuning range of (a) DSG and (b) DCW BWOs for the beam voltage 15.8–17.8 and 11.75–13.3 kV, respectively.

dispersion curve. Machining tolerances are expected to be ± 1 μm, which is sufficient to achieve the desired performance.

Photolithographic techniques, such as UV-LIGA, are demonstrated suitable for the dimension accuracy required for the two SWSs considered. However, especially for a small number of pieces, the fabrication of the mold and the electroforming process is not convenient. Furthermore, a relevant effort to achieve a level of surface roughness better than the skin depth (about 110 nm at 0.346 THz) to reduce ohmic losses is required. CNC milling offers high flexibility and possibility of patterning the third dimension. The state-of-the-art prototype nano-CNC milling machine, developed by DTL, a subsidiary of DMG-Mori-Seki, permits one to achieve performance at the state of the art, with reduced cost and high repeatability for dimensions suitable for THz regime structures [10]. The high accuracy of the nanomilling machine was proved to obtain levels of surface roughness down to 40 nm, well below the skin depth at 0.346 THz. The NN1000 nano/micromilling machine has a maximum spindle speed of 50 000 r/min; the chip load is kept below 0.001-mm feed per tool flute rpm. The proper setting of the machining parameters is fundamental in achieving excellent surface finish and tool lifetime.

In the case of the DSG and the DGW at 0.346 THz, the dimensions shown in Table I represent a formidable fabrication challenge. A test of feasibility for the fabrication was performed realizing the DSG and the DCW in aluminum

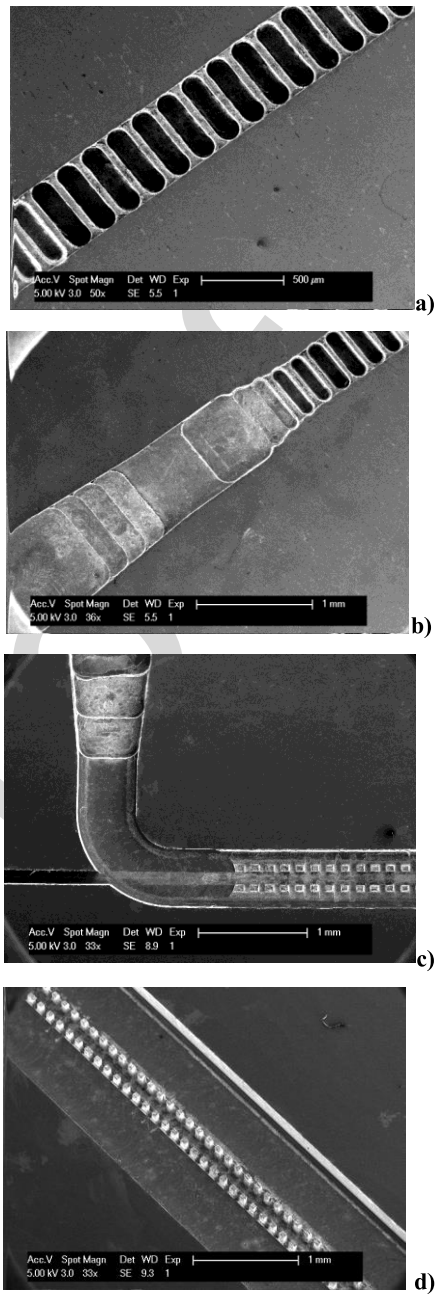

Fig. 11. SEM images of the SWSs fabricated by nano-CNC milling. (a) and (b) DSG. (c) and (d) DCW.

with the dimensions shown in Table I. Four different SEM views of the DSG and the DCW realized by nano-CNC milling are shown in Fig. 11. The high level of accuracy for the very small dimensions is readily observed. The high definition of the pillars is notable. Due to the characteristics of aluminum, the surface roughness achieved was higher than expected. The fabricated samples were primarily built to test the microfabrication process in terms of dimensions achieved. However, the measurements of the S-parameters were carried out. The setup for the DSG measurement is shown in Fig. 12. It consists of two halves assembled together by a system of alignment pins. The setup for the DCW is similar to a lid to close the waveguide that does not require a very accurate alignment procedure.

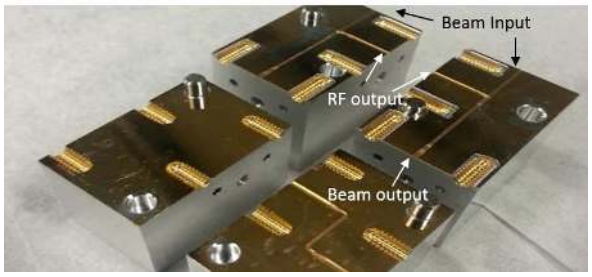

Fig. 12. Full DSG assembly with alignment pins and flanges.

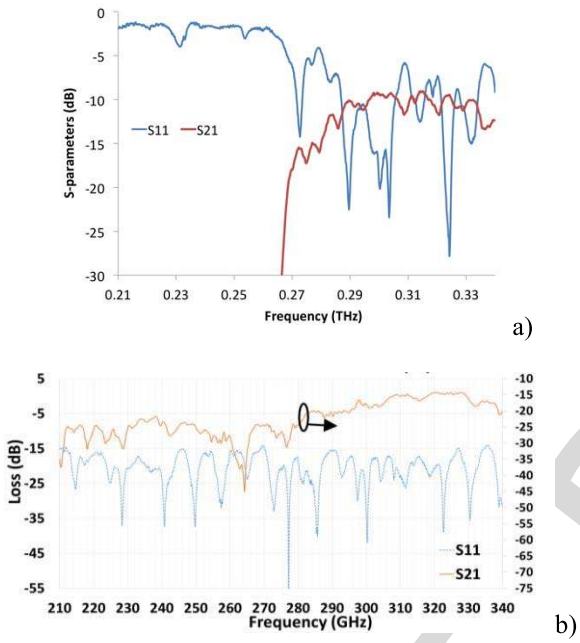

Fig. 13. Measurements of the S-parameters of (a) DCW and (b) DSG in the low range of the band.

The S-parameters of the fabricated structures were measured. The S_{11} and S_{21} for the fabricated DSG and DCW are shown in Fig. 13(a) and (b), respectively. The measurements are limited to the range of frequency below 0.34 THz due to the available frequency range of the vector network analyzer. The relatively high value of the transmission losses (S_{21}) is due to the difficulty to machining aluminum in this initial fabrication test. An improved surface will be obtained by the use of a different tooling and replacing aluminum with copper. The transmission parameter of the DSG circuit is lower than what was predicted in simulation models, and this is due to poor surface roughness. The first DSG grating circuit has surface roughness with R_a (arithmetic mean surface roughness) of about 500 nm, and it is expected that this can be improved to well below 100 nm by implementing diamond tooling. However, the fabricated samples demonstrated the CNC milling as a suitable process for SWS in the sub-THz range.

VI. Gun and Window

The design of the electron gun for the cylindrical beam is based on a conventional Pierce gun and does not present specific novelty. On the contrary, the sheet beam requires an accurate design of the gun and the magnetic focusing system.

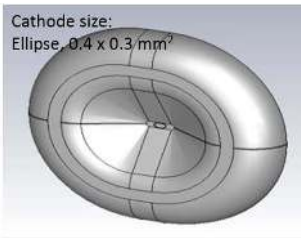

Fig. 14. Electron gun schematic.

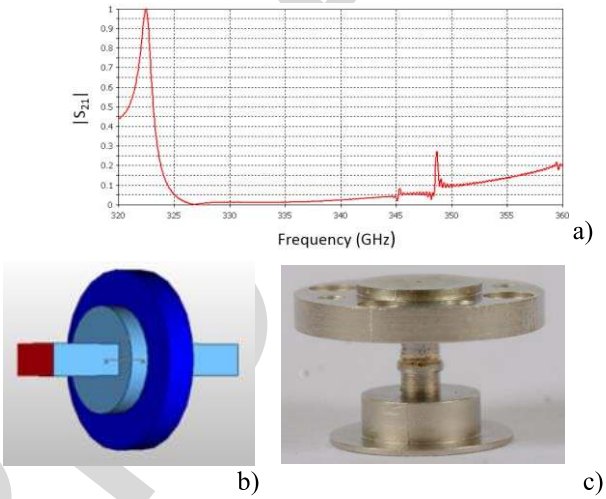

Fig. 15. 0.346-THz window. (a) Simulated S-parameter (S_{21}). (b) Schematic. (c) Prototype.

A planar cathode is considered to generate the cylindrical electron beam. A preliminary simulation and test was performed, where a beam voltage of 17.4 kV and a current of 14 mA have been obtained. The elliptical electron beam has a ratio 5.4:1 with a current density of 94 A/cm^2 and a 50% fill factor [6]. The schematic for the gun is shown in Fig. 14.

Different solutions of magnetic focusing systems based on solenoidal structures are under investigation to obtain up to 1.3 T for the full length of the DSG BWO. Based on PIC analysis performed in CST, 98.5% beam transmission efficiency is expected. The solenoid magnet structure has a radial component of magnetic field of 1.3 T and a longitudinal component of 0.35 T. External dimensions of the magnetic structure are 62 × 32 × 35.4 mm^3. Engineering estimates predict that the weight of the full system, including magnets, will be under 10 pounds.

A window, suitable for both the DSG and DWG BWOs, was designed and simulated using CST MWS [Fig. 15(a)] and tested in the frequency range 327–347 GHz. The window is a pillbox-type with MPCVD diamond as the disk. The MVCVP diamond dielectric constant is 5.6 with the loss tangent of 0.003 in the simulation. The thickness of the disk is 0.3 mm, the diameter is 2 mm, and the depth and the diameter of the circular waveguides are 0.7 and 1.2 mm, respectively. The flange connecting the internal SWS and the outer load is WR2.8 rectangular waveguide. Further refinements are

in progress. Fig. 15(b) and (c) shows the schematic and a first prototype of the window, respectively.

VII. Conclusion

An international collaboration of leading institutions in vacuum electronics in China, the U.K., and the U.S. is working on building a new family of THz vacuum electron devices for medium power generation. The availability of these sources will permit to enable a new high-k plasma diagnostic to improve the understanding of plasma turbulence in nuclear fusion reactor and many other applications in the THz range. Two different topologies of SWSs have been adopted to design the 0.346-THz BWOs. The DSG and the DCW have been demonstrated to be suitable interaction structures to provide a wide range of performance, with a tailored design. The fabrication of the SWS is a formidable challenge. The samples realized by CNC milling have proved the high accuracy of the process.

The fabrication of all the parts for the final assembly of the BWOs is in progress.

References

[1] P. H. Siegel, "Terahertz technology," *IEEE Trans. Microw. Theory Techn.*, vol. 50, no. 3, pp. 910–928, Mar. 2002.

[2] G. Chattopadhyay, "Technology, capabilities, and performance of low power terahertz sources," *IEEE Trans. THz Sci. Technol.*, vol. 1, no. 1, pp. 33–53, Sep. 2011.

[3] J. H. Booske *et al.*, "Vacuum electronic high power terahertz sources," *IEEE Trans. THz Sci. Technol.*, vol. 1, no. 1, pp. 54–75, Sep. 2011.

[4] M. Mineo and C. Paoloni, "Corrugated rectangular waveguide tunable backward wave oscillator for terahertz applications," *IEEE Trans. Electron Devices*, vol. 57, no. 6, pp. 1481–1484, Jun. 2010.

[5] Y.-M. Shin, D. Gamzina, L. R. Barnett, F. Yaghmaie, A. Baig, and N. C. Luhmann, Jr., "UV lithography and molding fabrication of ultrathick micrometallic structures using a KMPR photoresist," *J. Microelectromech. Syst.*, vol. 19, no. 3, pp. 683–689, Jun. 2010.

[6] A. Baig *et al.*, "MEMS vacuum electronics," in *Encyclopedia of Nanotechnology*. Berlin, Germany: Springer-Verlag, 2012, pp. 1359–1368.

[7] C. Paoloni *et al.*, "Design and realization aspects of 1-THz cascade backward wave amplifier based on double corrugated waveguide," *IEEE Trans. Electron Devices*, vol. 60, no. 3, pp. 1236–1243, Mar. 2013.

[8] R. Letizia, M. Mineo, and C. Paoloni, "Photonic crystal-structures for THz vacuum electron devices," *IEEE Trans. Electron Devices*, vol. 62, no. 1, pp. 178–183, Jan. 2015.

[9] J. C. Tucek *et al.*, "A 100 mW, 0.670 THz power module," in *Proc. IEEE 13th Int. Vac. Electron. Conf. (IVEC)*, Apr. 2012, pp. 31–32.

[10] R. Barchfeld, D. Gamzina, A. Baig, L. R. Barnett, and N. C. Luhmann, Jr., "Nano CNC milling of two different designs of 0.22 THz TWT circuits," in *Proc. IEEE 13th Int. Vac. Electron. Conf. (IVEC)*, Apr. 2012, pp. 549–550.

[11] J. Zhao *et al.*, "High current density and long-life nanocomposite scandate dispenser cathode fabrication," *IEEE Trans. Electron Devices*, vol. 58, no. 4, pp. 1221–1228, Apr. 2011.

[12] J. Q. Dong, H. Sanuki, K. Itoh, and L. Chen, "Electron temperature gradient instability in toroidal plasmas," *Phys. Plasmas*, vol. 9, no. 11, pp. 4699–4708, 2002.

[13] Y. Ren *et al.*, "Experimental study of parametric dependence of electron-scale turbulence in a spherical tokamak," *Phys. Plasmas*, vol. 19, no. 5, p. 056125, 2012.

[14] D. R. Smith, E. Mazzucato, W. Lee, H. K. Park, C. W. Domier, and N. C. Luhmann, Jr., "A collective scattering system for measuring electron gyroscale fluctuations on the national spherical torus experiment," *Rev. Sci. Instrum.*, vol. 79, no. 12, p. 123501, 2008.

[15] Y. Ren *et al.*, "Density gradient stabilization of electron temperature gradient driven turbulence in a spherical tokamak," *Phys. Rev. Lett.*, vol. 106, no. 16, p. 165005, Apr. 2011.

[16] C. Paoloni *et al.*, "THz backward-wave oscillators for plasma diagnostic in nuclear fusion," in *Proc. IEEE Int. Conf. Plasma Sci. (ICOPS)*, May 2015, p. 1.

[17] Y.-M. Shin, L. R. Barnett, and N. C. Luhmann, Jr., "Strongly confined plasmonic wave propagation through an ultrawideband staggered double grating waveguide," *Appl. Phys. Lett.*, vol. 93, no. 22, p. 221504, 2008.

[18] M. Mineo and C. Paoloni, "Double-corrugated rectangular waveguide slow-wave structure for terahertz vacuum devices," *IEEE Trans. Electron Devices*, vol. 57, no. 11, pp. 3169–3175, Nov. 2010.

[19] CST AG, Darmstadt, Germany. *CST Studio Suite*. [Online]. Available: http://www.cst.com

[20] B. Goplen, L. Ludeking, D. Smith, and G. Warren, "User-configurable MAGIC for electromagnetic PIC calculations," *Comput. Phys. Commun.*, vol. 87, nos. 1–2, pp. 54–86, May 1995.

AQ:7

Claudio Paoloni (M'86–SM'11) received the Laurea degree in electronics engineering from the University of Rome Sapienza, Rome, Italy, in 1984.

He has been a Professor of Electronics with the Department of Engineering, Lancaster University, Lancaster, U.K., since 2012, where he is currently the Head of the Engineering Department.

Diana Gamzina received the B.S. degrees in mechanical engineering and materials science and the M.S. degree in mechanical engineering, in 2008 and 2012, respectively, and the Ph.D. degree with a focus on the thermomechanical design and analysis of high power and high frequency vacuum electronics.

She has been a Staff Member with the Millimeter-Wave Research Group, University of California at Davis, Davis, CA, USA, since 2008.

Logan Himes received the B.S. degrees in biotechnology and applied microbiology from the University of California at Davis (UC Davis), Davis, CA, USA, in 2010.

He has been an Associate Development Engineer with the Millimeter-Wave Research Group, UC Davis, since 2010, where he has been involved in the development of precision and high performance micro and nanomachining and manufacturing strategies and techniques for the production of high frequency vacuum electronics.

Branko Popovic is currently pursuing the Ph.D. degree with the Department of Electrical and Computer Engineering, University of California at Davis (UC Davis), Davis, CA, USA.

He is a member of the Millimeter-Wave Research Center with UC Davis. His current research interests include millimeter-wave vacuum electronics, under the guidance of Prof. N. Luhmann, with a main focus on the design of vacuum electronic devices using electromagnetic and particle in cell codes, and laboratory testing of these devices and related components.

Robert Barchfeld is currently pursuing the Ph.D. degree with the Department of Applied Science, University of California at Davis, Davis, CA, USA.

His current research interests include plasma physics and fusion technology under the guidance of Prof. N. Luhmann, the design, construction, and implementation of plasma diagnostic instruments, vacuum electronics, microfabrication, and related millimeter-wave technologies.

Lingna Yue, photograph and biography not available at the time of publication.

AQ:8

AQ:9

AQ:10

Yuan Zheng, photograph and biography not available at the time of publication.

Xiaopin Tang, photograph and biography not available at the time of publication.

Ye Tang, photograph and biography not available at the time of publication.

Pan Pan received the B.S. degree in engineering from Tsinghua University, Beijing, China, in 2010, and the M.S. degree in physical electronics from the Beijing Vacuum Electronics Research Institute (BVERI), Beijing, in 2015.

He joined BVERI in 2010, as an Assistant Engineer, where he is involved in developing W-band TWTs.

Hanyan Li, photograph and biography not available at the time of publication.

Rosa Letizia (M'13) received the Ph.D. degree in computational photonics from the University of Leeds, Leeds, U.K., in 2009.

She has been a Lecturer with the Engineering of Microwave, Terahertz and Light Group, Engineering Department, Lancaster University, Lancaster, U.K., and the Cockcroft Institute, Warrington, U.K., since 2011.

Mauro Mineo received the Ph.D. degree in telecommunication and microelectronic engineering from the University of Rome Tor Vergata, Rome, Italy.

He was a Research Associate with the Engineering Department, Lancaster University, Lancaster, U.K., from 2012 to 2015. He has been with e2v Technologies Ltd., Chelmsford, U.K., since 2015, as an RF/Microwave Modeling Engineer.

Jinjun Feng (M'94–SM'06) is currently the Vice Chief-Engineer and the Head of the Vacuum Electronics National Laboratory with the Beijing Vacuum Electronic Research Institute, Beijing, China. He has authored or co-authored one book, one book chapter, and over 200 papers in domestic and overseas conference proceedings and scientific journals.

Mr. Feng has been a fellow of the Chinese Institute of Electronics since 2013 and a member of the IEEE Electron Devices Society of the Vacuum Electronic Technical Committee since 2010. He was the Chair of the IEEE Electron Devices Society Beijing Chapter from 2011 to 2012, and he has been the Chair of the IEEE Beijing Section since 2014.

Neville C. Luhmann, Jr. (F'–) received the Ph.D. degree from the University of Maryland at College Park, College Park, MD, USA, in 1972. AQ:11

He is currently a Distinguished Professor with the Department of Electrical and Computer Engineering, University of California at Davis, Davis, CA, USA, where he is also a Co-Director of the Millimeter-Wave Research Center.

AUTHOR QUERIES

AUTHOR PLEASE ANSWER ALL QUERIES

PLEASE NOTE: Please note that we cannot accept new source files as corrections for your paper. If possible, please annotate the PDF proof we have sent you with your corrections and upload it via the Author Gateway. Alternatively, you may send us your corrections in list format. You may also upload revised graphics via the Author Gateway.

AQ:1 = Please confirm whether the edits made in the financial section are OK.
AQ:2 = Please confirm the postal codes for "Lancaster University, University of Electronic Science and Technology of China, Beijing Vacuum Electronic Research Institute, e2v Technologies Ltd."
AQ:3 = Please confirm the organization name "Beijing Vacuum Electronic Research Institute." And company name "e2v Technologies Ltd."
AQ:4 = Please provide the expansions for the acronyms "MEMS, CNC, MPCVD, and DTL."
AQ:5 = Please provide the captions for "Tables I and II."
AQ:6 = In Fig. 4, text is too small and difficult to read. Please provide clearer assembled image with more legible text.
AQ:7 = Please confirm the title and also provide the accessed date for ref. [19].
AQ:8 = Please provide the university name for the degrees received for the author "Diana Gamzina."
AQ:9 = Please confirm whether the edits made in the sentence "His current research … related components." are OK.
AQ:10 = Please confirm whether the edits made in the sentence "His current research … millimeter-wave technologies." are OK.
AQ:11 = Please provide the membership year for the author "Neville C. Luhmann."

THz Backward-Wave Oscillators for Plasma Diagnostic in Nuclear Fusion

Claudio Paoloni, *Senior Member, IEEE*, Diana Gamzina, Logan Himes, Branko Popovic, Robert Barchfeld, Lingna Yue, Yuan Zheng, Xiaopin Tang, Ye Tang, Pan Pan, Hanyan Li, Rosa Letizia, *Member, IEEE*, Mauro Mineo, Jinjun Feng, *Senior Member, IEEE*, and Neville C. Luhmann, Jr., *Fellow, IEEE*

***Abstract*— Understanding of the anomalous transport attributed to short-scale length microturbulence through collective scattering diagnostics is key to the development of nuclear fusion energy. Signals in the subterahertz (THz) range (0.1–0.8 THz) with adequate power are required to map wider wavenumber regions. The progress of a joint international effort devoted to the design and realization of novel backward-wave oscillators at 0.346 THz and above with output power in the 1 W range is reported herein. The novel sources possess desirable characteristics to replace the bulky, high maintenance, optically pumped far-infrared lasers so far utilized in this plasma collective scattering diagnostic. The formidable fabrication challenges are described. The future availability of the THz source here reported will have a significant impact in the field of THz applications both for scientific and industrial applications, to provide the output power at THz so far not available.**

***Index Terms*— Backward-wave oscillator (BWO), double-corrugated waveguide (DCW), double-staggered grating (DSG), plasma diagnostic, terahertz (THz).**

I. Introduction

TERAHERTZ (THz) vacuum electron devices are gaining significant consideration when the generation of relatively high power in the frequency range below 1 THz is needed [1]–[9]. In particular, the backward-wave oscillator (BWO) is an effective solution to produce relatively high power and stable monochromatic THz signals. BWOs can be electronically tuned over a wide frequency range around the operating frequency and have high stability in frequency (up to 10^{-7} to 10^{-8} by phase locking). However, the only available BWOs are based on old technologies. No compact, affordable, and long-life THz BWOs is currently available.

Recently, the introduction of new high aspect-ratio fabrication processes derived from the MEMS technologies as the lithography, electroplating, and molding (LIGA) [5], [7] and advanced mechanical microfabrication as nano-CNC milling [10] provides an accuracy at the submicrometer level, which satisfies the demanding specifications of interaction structures or slow-wave structures (SWSs) to support the THz operation frequencies. Furthermore, the progress on simulation tools based on accurate 3-D electromagnetic and particle-in-cell (PIC) solvers permits now a reliable prediction of the THz vacuum source performance, to ease the fabrication phase. The development of innovative cathode materials [10] is leading to a novel generation of electron guns, with high current density and long lifetime, fundamental for the overall device mean time between failures and high-frequency stability. Nevertheless, the main challenges are to achieve a surface roughness below the skin depth (66 nm at 1 THz) for minimizing the ohmic losses and the assembly and alignment of the beam with tolerance in the order of tens of micrometers.

Nuclear fusion is one of the fields, where the availability of THz BWOs will have a relevant impact on improving the understanding of a critical phenomenon as the anomalous transport of the plasma. It still remains a fundamental area of investigation, which is essential for the development of fusion energy. The measurement technique is based on the collective Thomson scattering at THz frequency [12]–[15]. The plasma is illuminated by a THz beam that is scattered by the charged particles. The scattered beams due to the electron density fluctuations are detected by a receiver array and thereby map out the location, wavenumber spectrum, and strength of the turbulence.

In the recent upgrade of the high-k scattering system at NSTX experiment at Princeton, the wavenumber k_θ coverages, and it has been increased to target electron temperature gradient modes by increasing the probe frequency from 0.280 to 0.693 THz. The availability of solid-state sources is limited to about 0.3 THz and 30 mW, while about 100 mW are needed at 0.693 THz to excite a detectable scattering.

Manuscript received November 1, 2015; revised February 5, 2016; accepted March 9, 2016. This work was supported in part by the National Science Foundation through the Major Research Instrumentation Program under Grant CHE-1429258, in part by the U.S. Department of Energy, National Spherical Torus Experiment under Grant DE-FG02-99ER54518, in part by the U.S. Department of Defense under Grant M67854-06-1-5118, in part by the Defense Advanced Research Projects Agency, Defense Sciences Office, under Grant G8U543366, in part by the U.K. Engineering and Physical Sciences Research Council under Grant EP/L026597/1, and in part by the ATK's Alliance Partnership Program, which was provided via the use of their MAGIC software.

C. Paoloni and R. Letizia are with Lancaster University, Lancaster LA1 4YW, U.K. (e-mail: c.paoloni@lancaster.ac.uk; r.letizia@lancaster.ac.uk).

D. Gamzina, L. Himes, B. Popovic, R. Barchfeld, and N. C. Luhmann, Jr., are with the Department of Electrical and Computer Engineering, University of California at Davis, Davis, CA 95616 USA (e-mail: dgamzina@ucdavis.edu; lghimes@ucdavis.edu; bkpopovic@ucdavis.edu; rbarchfeld@ucdavis.edu; ncluhmann@ucdavis.edu).

L. Yue, Y. Zheng, and X. Tang are with the University of Electronic Science and Technology of China, Chengdu 610051, China (e-mail: lnyue@uestc.edu.cn; zyzheng@ucdavis.edu; xiaopintang@gmail.com).

Y. Tang, P. Pan, H. Li, and J. Feng are with the Vacuum Electronics National Laboratory, Beijing Vacuum Electronic Research Institute, Beijing 100016, China (e-mail: tangye1983@163.com; p-pan@hotmail.com; fengjinjun@tsinghua.org.cn).

M. Mineo is with e2v Technologies Ltd., Chelmsford CM1 2QU, U.K. (e-mail: m.mineo@e2v.com).

Color versions of one or more of the figures in this paper are available online at http://ieeexplore.ieee.org.

Digital Object Identifier 10.1109/TPS.2016.2541119

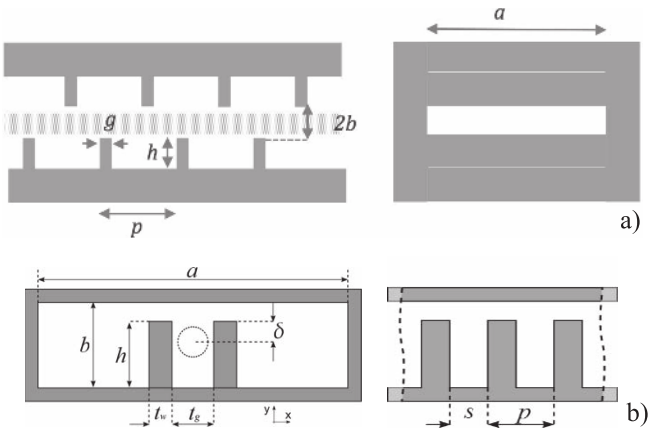

Fig. 1. SWS for 0.346-THz operation. (a) DSG. (b) DCW. The gray area in (a) and the dashed circle in (b) represent the sheet and cylindrical beam for the DSG and the DCW, respectively.

Presently, the only THz source to deliver ∼100 mW at 0.693 THz needed to provide the minimum scattered signal level to be detected by the receiver array is a bulky optically pumped far infrared. A second high-frequency source is needed to provide local oscillator (LO) power for the receiver array. The use of a second laser is not feasible. It has been chosen to use an array based on sensitive room temperature subharmonic mixers working roughly at half of the illumination source frequency, namely, 0.346 THz. It is required 3 to 5 mW of LO power per mixer.

This paper describes an international joint effort of three leading institutions in China, the U.K., and the U.S. to design and construct a novel family of BWOs, operating at the frequency of 0.346 THz, to satisfy the quest for LO power for the matrix array for the NSTX-U plasma diagnostic and other future plasma diagnostic systems [16]. The design target is to achieve an output power in the range of hundreds of milliwatt by lightweight, compact, affordable, low-operating cost BWOs to enable a wide matrix of receivers.

This paper is organized as follows. The properties of two different SWSs suitable for THz BWO fabrication are reported in Section II. Section III describes the design aspects and the cold parameters. Section IV details the hot simulations and performance of the two BWOs. Challenges involved with microfabrication technologies of the proposed BWOs are discussed in Section V. Section VI reports on the gun and the window.

II. Terahertz Slow-Wave Structures

At microwave frequencies, helices are the most common SWSs, but as the frequency increases toward the millimeter-wave range, their dimensions are too small for fabrication, and new geometries must be adopted. The simple structure of the rectangular corrugated waveguide inspired different structures that can be realized by the available fabrication processes with the dimensions to support THz frequencies.

In particular, the double-staggered grating (DSG) [17] [Fig. 1(a)] and the double-corrugated waveguide (DCW) [18] [Fig. 1(b)] are the two SWSs that have been successfully proposed for operation at THz frequencies and overcome the fabrication issues of the conventional structures.

The DSG is conceived to support an elliptical sheet electron beam. The advantage of the sheet electron beam is the large cross section that permits to deliver a high beam current using a relatively beam current density. The sheet beam requires a careful design of the magnetic focusing system, but it is very promising to realize high-power vacuum electron devices by using low cathode loading guns.

The DCW is conceived to support a cylindrical electron beam. The DCW is of easy fabrication and assembly. The advantage of a cylindrical electron beam is that it is generated by the well-established Pierce gun technology and focused by the use of a conventional magnetic focusing system.

Both the SWSs are very promising to realize THz BWOs with a wide range of characteristics in terms of fabrication, output power, and cost.

III. BWO Design

The approach of using two different SWSs, the DSG and the DCW, to design a family of THz BWO is a breakthrough for tailored power generation at THz frequencies. Two BWOs based on the DSG and the DCW will be the first two devices for a new family of THz sources to cover a wide range of applications.

The main design targets are given in the following:

1) low cost;
2) easy assembly for high yield;
3) compact dimensions (200–300 cm^3);
4) wide range of performance to potentially cover the sub-THz spectrum (0.1–1 THz);
5) tunable (at least 5%);
6) low beam voltage and compact power supply.

A 0.346-THz operating frequency is considered in the following for application in the plasma diagnostic in nuclear fusion, as described in Section I. The first design parameter defined was the beam voltage that determines the length of the period of the SWSs. A low beam voltage in the range of 12–18 kV favors to use of a compact and low-cost power supply. The resulting period was estimated to be in the range of the fabrication process.

Due to the different structures, different beam voltages were adopted. The DSG was designed to operate with 17-kV beam voltage, while the DCW was to support about 13 kV. The dimensions of the two SWSs are shown in Table I. It is notable that a period shorter than 200 μm is required. In Fig. 2, the dispersion curve of the DCW with superimposed beam line at 12.8 kV is shown. The interaction impedance is typically low in the backward-wave mode.

1) Couplers: A detailed study based on 3-D electromagnetic simulation [18] on the coupler to transform the mode in the SWS in the TE_{10} at the flange at the output port was carried out to maximize power transfer. The conductivity of copper considered in simulation is $\sigma_{cu} = 3.9 \times 10^7$ S/m [7]. The coupler is a three-port network; one port is connected to the SWS, a second port is the beam tunnel to connect the gun, and the third port is the output port connected to the flange.

AQ:5

TABLE I

DSG		DCW	
Parameter	µm	Parameter	µm
a	483	a	1500
b	45	b	200
h	170	h	140
p	185	p	140
g	44	s	80
		t_g	120
		t_w	60

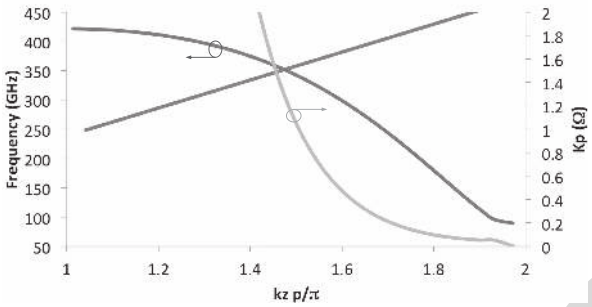

Fig. 2. DCW dispersion curve (brown curve), interaction impedance (orange curve), and beam line at 12.8 kV (blue line).

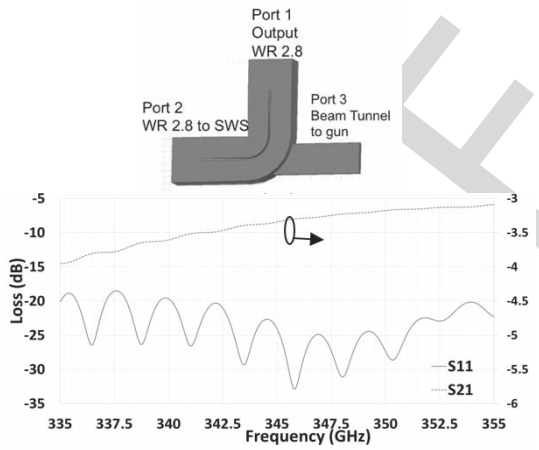

Fig. 3. DSG coupler S-parameters.

The coupler for the DSG is particularly challenging due to the wide beam tunnel needed for the sheet beam. Having a low cutoff frequency in the same range of the SWS, a ridge is added to the bend (Fig. 3) to perturb the matching between the SWS and the beam tunnel. The resulting S_{11} is better than -25 dB over a wide frequency range around 0.346 THz.

A study of the coupler for the DCW was performed by considering a back-to-back structure. First, a simple structure including a tapered transition between a waveguide with the same cross section of the DWG and the flanges is designed, as shown in Fig. 4(a), to evaluate the effect of the

replace all

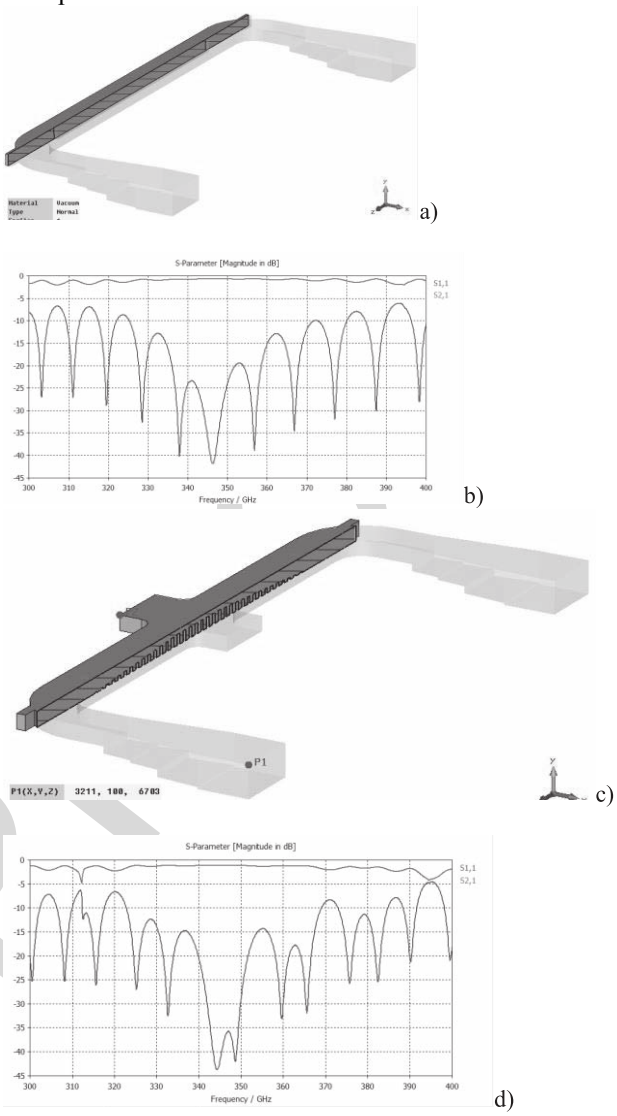

Fig. 4. DCW coupler. (a) Waveguide without DCW. (b) S-parameter structure. (c) Waveguide with DCW. (d) S-parameters.

AQ:6

waveguide tapering. Fig. 4(b) shows the obtained S_{11} better than -25 dB in the operation range. Next, a second structure with similar topology, including three sections of pillars (two tapered sections and one short section with a nominal height), is designed for the best matching, as shown in Fig. 4(c). Results show that S_{11} in this case is better than -35 dB in the region around the operating frequency [Fig. 4(d)].

Both the couplers' performance ensures the efficient propagation of the RF signal from the interaction structure to the flanges.

IV. Large Signal Simulations

The design of the two BWOs is based on the definition of the critical length for oscillations to set a proper number of periods within the SWS. Results from this optimization process are shown in Table II.

Next, the 3-D PIC simulations performed to evaluate the electrical behavior of the BWOs. The DSG BWO supports an

TABLE II

BWO specifications	DSG	DCW
Beam Voltage	17.1 kV	12.8 kV
Beam current	14 mA	10 mA
Beam channel	483 x 90 μm	120 μm
Beam Aspect Ratio	5.4 : 1	Round
Beam Current Density	160 A/cm^2	127 A/cm^2
Magnetic field	0.35 T	0.5 T
No. Periods	65	116
Total length	~ 15 mm	~ 20 mm

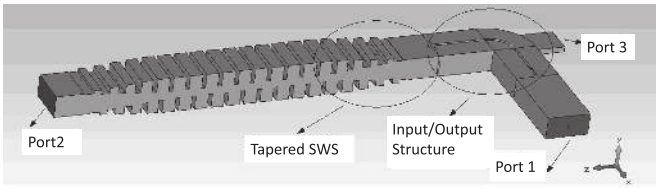

Fig. 5. PIC simulation setup for the DSG BWO.

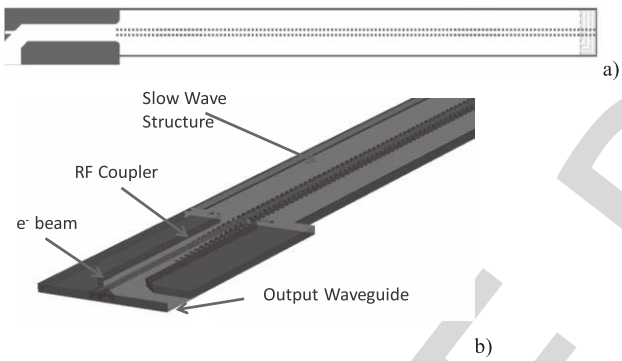

Fig. 6. PIC simulation setup for the DCW PIC simulations. (a) Top view. (b) Coupler detail.

elliptical electron beam with the cross section of $400 \times 50\ \mu m^2$ and the current of 14 mA (the aspect ratio of 5.4:1). The DWC BWO supports a cylindrical electron beam of 50-μm radius and 10-mA current. Due to the different beam parameters used, the overall device performance is different for the two BWOs and should be evaluated in the context of the different technological challenges required and the different application needs. The DSG BWO is modeled by CST Particle Studio [19] (simulation setup in Fig. 5) and the DCW BWO is modeled by MAGIC3D [20] (simulation setup in Fig. 6).

The results of output power for the two devices are shown in Fig. 7. The DSG BWO [Fig. 7(a)] provides about 1 W and the DCW BWO about 0.4 W [Fig. 7(b)]. The electron energy distribution along the longitudinal direction for both the BWOs is shown in Fig. 8. The spectral response at the output port of the DCW BWO is shown in Fig. 9, showing the highly monochromatic generation of signal at the frequency of interest.

In order to demonstrate the tunability of the BWO designs, the tuning range for the DSG and the DCW is shown in Fig. 10(a) and (b), respectively. It can be noted that a

to replace

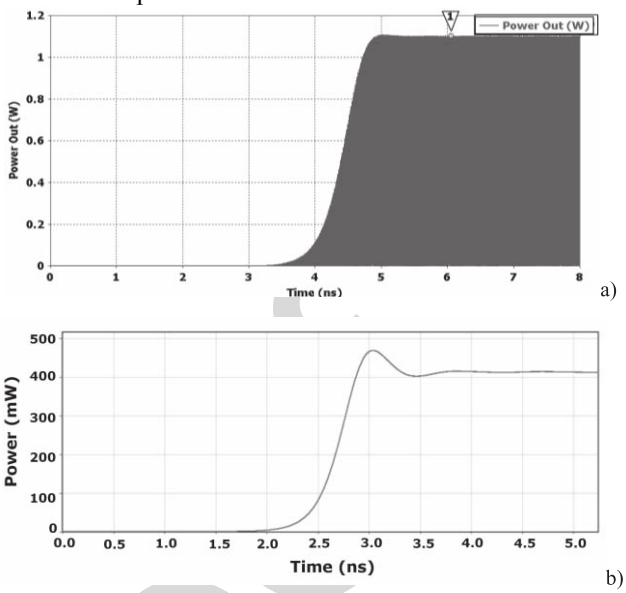

Fig. 7. Average output power for (a) DSG and (b) DCW BWOs.

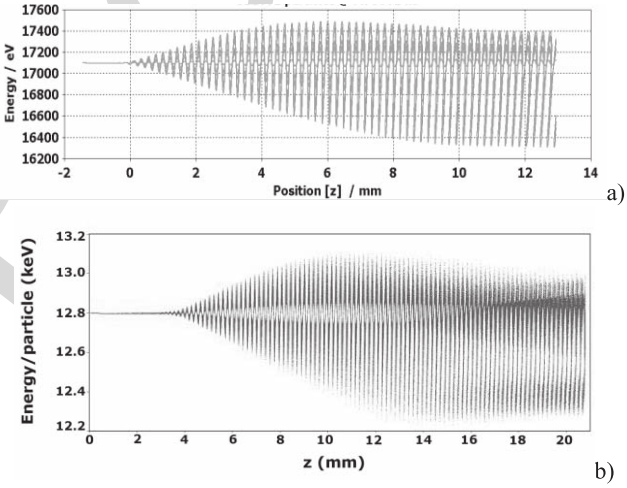

Fig. 8. Electron energy. (a) DSG BWO. (b) DCW BWO.

variation of beam voltage in the range of 15.8–17.8 kV permits a variation in frequency of 12 GHz for the DSG and that the same relative change in the nominal beam voltage allows a tuning of 14 GHz for the DCW.

The BWO performances so far presented are at the state of the art. The high power level and tuning features, not achievable by any other technology today, represent a breakthrough in the field.

V. BWO Microfabrication

The main challenge in the THz frequency range is the fabrication of SWSs with the expected electromagnetic behavior while establishing a reliable and repeatable process. For the DSG circuit, vane height is the most sensitive dimension which determines the bandwidth of the device. The period of the structure affects the central operating frequency, whereas the width of the DSG controls the dispersion curve. The DCW structure is more sensitive to the h and p values driving the

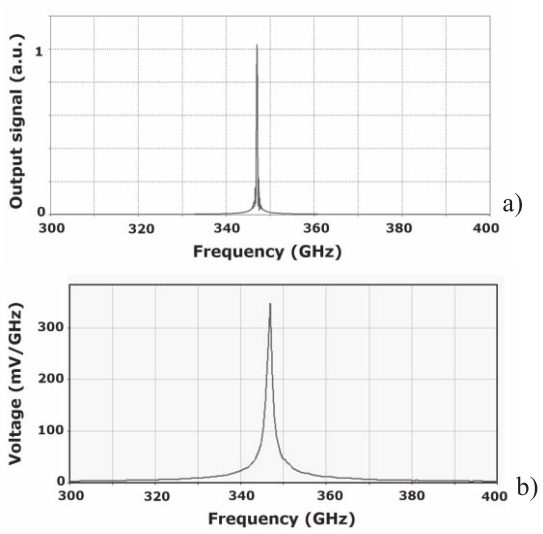

Fig. 9. Spectrum of (a) DSG and (b) DCW BWOs.

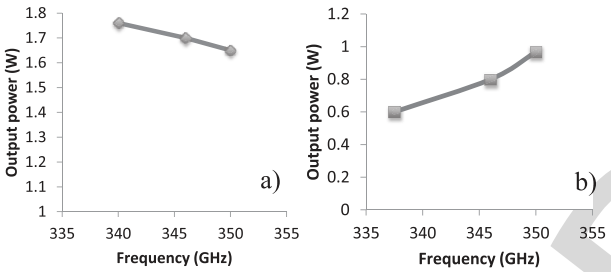

Fig. 10. Instantaneous power and tuning range of (a) DSG and (b) DCW BWOs for the beam voltage 15.8–17.8 and 11.75–13.3 kV, respectively.

dispersion curve. Machining tolerances are expected to be ± 1 μm, which is sufficient to achieve the desired performance.

Photolithographic techniques, such as UV-LIGA, are demonstrated suitable for the dimension accuracy required for the two SWSs considered. However, especially for a small number of pieces, the fabrication of the mold and the electroforming process is not convenient. Furthermore, a relevant effort to achieve a level of surface roughness better than the skin depth (about 110 nm at 0.346 THz) to reduce ohmic losses is required. CNC milling offers high flexibility and possibility of patterning the third dimension. The state-of-the-art prototype nano-CNC milling machine, developed by DTL, a subsidiary of DMG-Mori-Seki, permits one to achieve performance at the state of the art, with reduced cost and high repeatability for dimensions suitable for THz regime structures [10]. The high accuracy of the nanomilling machine was proved to obtain levels of surface roughness down to 40 nm, well below the skin depth at 0.346 THz. The NN1000 nano/micromilling machine has a maximum spindle speed of 50 000 r/min; the chip load is kept below 0.001-mm feed per tool flute rpm. The proper setting of the machining parameters is fundamental in achieving excellent surface finish and tool lifetime.

In the case of the DSG and the DGW at 0.346 THz, the dimensions shown in Table I represent a formidable fabrication challenge. A test of feasibility for the fabrication was performed realizing the DSG and the DCW in aluminum

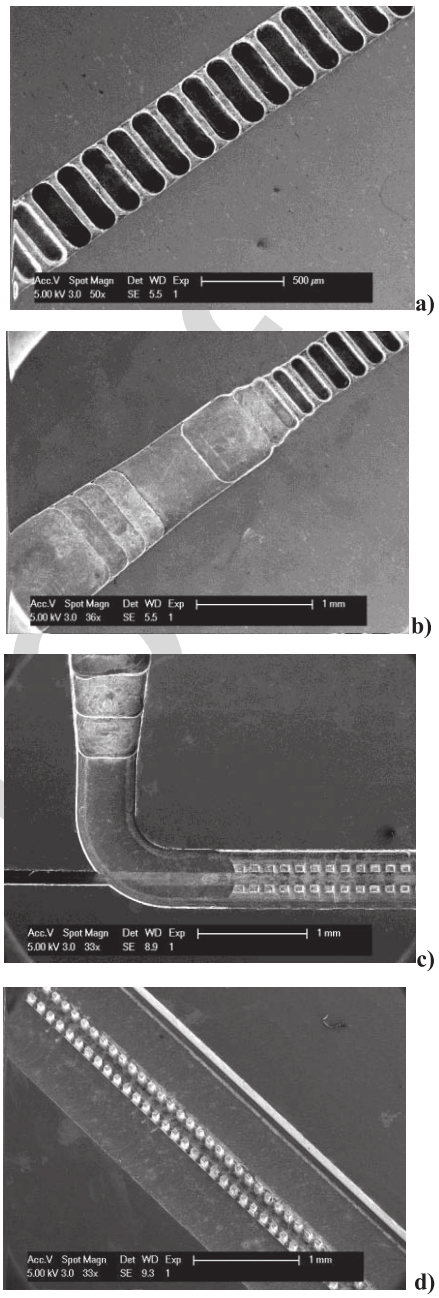

Fig. 11. SEM images of the SWSs fabricated by nano-CNC milling. (a) and (b) DSG. (c) and (d) DCW.

with the dimensions shown in Table I. Four different SEM views of the DSG and the DCW realized by nano-CNC milling are shown in Fig. 11. The high level of accuracy for the very small dimensions is readily observed. The high definition of the pillars is notable. Due to the characteristics of aluminum, the surface roughness achieved was higher than expected. The fabricated samples were primarily built to test the microfabrication process in terms of dimensions achieved. However, the measurements of the S-parameters were carried out. The setup for the DSG measurement is shown in Fig. 12. It consists of two halves assembled together by a system of alignment pins. The setup for the DCW is similar to a lid to close the waveguide that does not require a very accurate alignment procedure.

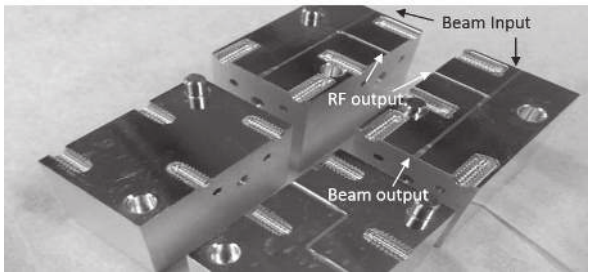

Fig. 12. Full DSG assembly with alignment pins and flanges.

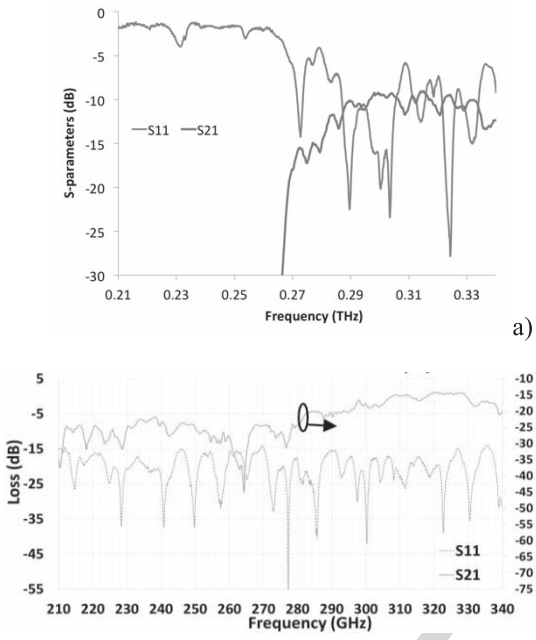

Fig. 13. Measurements of the S-parameters of (a) DCW and (b) DSG in the low range of the band.

The S-parameters of the fabricated structures were measured. The S_{11} and S_{21} for the fabricated DSG and DCW are shown in Fig. 13(a) and (b), respectively. The measurements are limited to the range of frequency below 0.34 THz due to the available frequency range of the vector network analyzer. The relatively high value of the transmission losses (S_{21}) is due to the difficulty to machining aluminum in this initial fabrication test. An improved surface will be obtained by the use of a different tooling and replacing aluminum with copper. The transmission parameter of the DSG circuit is lower than what was predicted in simulation models, and this is due to poor surface roughness. The first DSG grating circuit has surface roughness with R_a (arithmetic mean surface roughness) of about 500 nm, and it is expected that this can be improved to well below 100 nm by implementing diamond tooling. However, the fabricated samples demonstrated the CNC milling as a suitable process for SWS in the sub-THz range.

VI. Gun and Window

The design of the electron gun for the cylindrical beam is based on a conventional Pierce gun and does not present specific novelty. On the contrary, the sheet beam requires an accurate design of the gun and the magnetic focusing system.

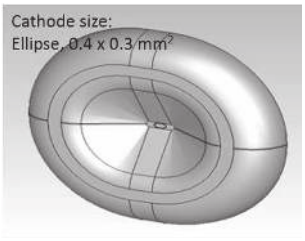

Fig. 14. Electron gun schematic.

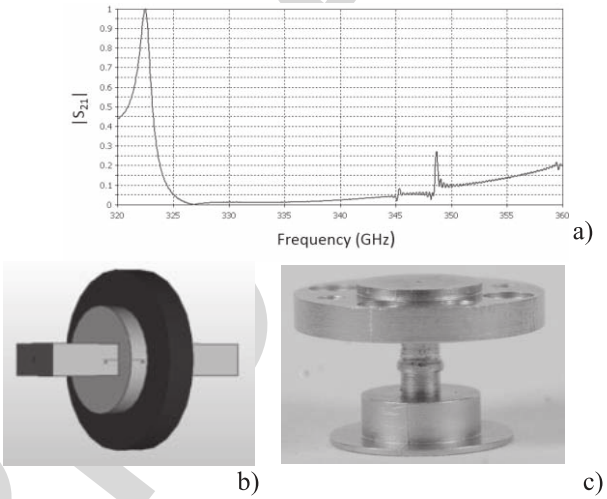

Fig. 15. 0.346-THz window. (a) Simulated S-parameter (S_{21}). (b) Schematic. (c) Prototype.

A planar cathode is considered to generate the cylindrical electron beam. A preliminary simulation and test was performed, where a beam voltage of 17.4 kV and a current of 14 mA have been obtained. The elliptical electron beam has a ratio 5.4:1 with a current density of 94 A/cm^2 and a 50% fill factor [6]. The schematic for the gun is shown in Fig. 14.

Different solutions of magnetic focusing systems based on solenoidal structures are under investigation to obtain up to 1.3 T for the full length of the DSG BWO. Based on PIC analysis performed in CST, 98.5% beam transmission efficiency is expected. The solenoid magnet structure has a radial component of magnetic field of 1.3 T and a longitudinal component of 0.35 T. External dimensions of the magnetic structure are 62 × 32 × 35.4 mm^3. Engineering estimates predict that the weight of the full system, including magnets, will be under 10 pounds.

A window, suitable for both the DSG and DWG BWOs, was designed and simulated using CST MWS [Fig. 15(a)] and tested in the frequency range 327–347 GHz. The window is a pillbox-type with MPCVD diamond as the disk. The MVCVP diamond dielectric constant is 5.6 with the loss tangent of 0.003 in the simulation. The thickness of the disk is 0.3 mm, the diameter is 2 mm, and the depth and the diameter of the circular waveguides are 0.7 and 1.2 mm, respectively. The flange connecting the internal SWS and the outer load is WR2.8 rectangular waveguide. Further refinements are

in progress. Fig. 15(b) and (c) shows the schematic and a first prototype of the window, respectively.

VII. Conclusion

An international collaboration of leading institutions in vacuum electronics in China, the U.K., and the U.S. is working on building a new family of THz vacuum electron devices for medium power generation. The availability of these sources will permit to enable a new high-k plasma diagnostic to improve the understanding of plasma turbulence in nuclear fusion reactor and many other applications in the THz range. Two different topologies of SWSs have been adopted to design the 0.346-THz BWOs. The DSG and the DCW have been demonstrated to be suitable interaction structures to provide a wide range of performance, with a tailored design. The fabrication of the SWS is a formidable challenge. The samples realized by CNC milling have proved the high accuracy of the process.

The fabrication of all the parts for the final assembly of the BWOs is in progress.

References

[1] P. H. Siegel, "Terahertz technology," *IEEE Trans. Microw. Theory Techn.*, vol. 50, no. 3, pp. 910–928, Mar. 2002.

[2] G. Chattopadhyay, "Technology, capabilities, and performance of low power terahertz sources," *IEEE Trans. THz Sci. Technol.*, vol. 1, no. 1, pp. 33–53, Sep. 2011.

[3] J. H. Booske *et al.*, "Vacuum electronic high power terahertz sources," *IEEE Trans. THz Sci. Technol.*, vol. 1, no. 1, pp. 54–75, Sep. 2011.

[4] M. Mineo and C. Paoloni, "Corrugated rectangular waveguide tunable backward wave oscillator for terahertz applications," *IEEE Trans. Electron Devices*, vol. 57, no. 6, pp. 1481–1484, Jun. 2010.

[5] Y.-M. Shin, D. Gamzina, L. R. Barnett, F. Yaghmaie, A. Baig, and N. C. Luhmann, Jr., "UV lithography and molding fabrication of ultrathick micrometallic structures using a KMPR photoresist," *J. Microelectromech. Syst.*, vol. 19, no. 3, pp. 683–689, Jun. 2010.

[6] A. Baig *et al.*, "MEMS vacuum electronics," in *Encyclopedia of Nanotechnology*. Berlin, Germany: Springer-Verlag, 2012, pp. 1359–1368.

[7] C. Paoloni *et al.*, "Design and realization aspects of 1-THz cascade backward wave amplifier based on double corrugated waveguide," *IEEE Trans. Electron Devices*, vol. 60, no. 3, pp. 1236–1243, Mar. 2013.

[8] R. Letizia, M. Mineo, and C. Paoloni, "Photonic crystal-structures for THz vacuum electron devices," *IEEE Trans. Electron Devices*, vol. 62, no. 1, pp. 178–183, Jan. 2015.

[9] J. C. Tucek *et al.*, "A 100 mW, 0.670 THz power module," in *Proc. IEEE 13th Int. Vac. Electron. Conf. (IVEC)*, Apr. 2012, pp. 31–32.

[10] R. Barchfeld, D. Gamzina, A. Baig, L. R. Barnett, and N. C. Luhmann, Jr., "Nano CNC milling of two different designs of 0.22 THz TWT circuits," in *Proc. IEEE 13th Int. Vac. Electron. Conf. (IVEC)*, Apr. 2012, pp. 549–550.

[11] J. Zhao *et al.*, "High current density and long-life nanocomposite scandate dispenser cathode fabrication," *IEEE Trans. Electron Devices*, vol. 58, no. 4, pp. 1221–1228, Apr. 2011.

[12] J. Q. Dong, H. Sanuki, K. Itoh, and L. Chen, "Electron temperature gradient instability in toroidal plasmas," *Phys. Plasmas*, vol. 9, no. 11, pp. 4699–4708, 2002.

[13] Y. Ren *et al.*, "Experimental study of parametric dependence of electron-scale turbulence in a spherical tokamak," *Phys. Plasmas*, vol. 19, no. 5, p. 056125, 2012.

[14] D. R. Smith, E. Mazzucato, W. Lee, H. K. Park, C. W. Domier, and N. C. Luhmann, Jr., "A collective scattering system for measuring electron gyroscale fluctuations on the national spherical torus experiment," *Rev. Sci. Instrum.*, vol. 79, no. 12, p. 123501, 2008.

[15] Y. Ren *et al.*, "Density gradient stabilization of electron temperature gradient driven turbulence in a spherical tokamak," *Phys. Rev. Lett.*, vol. 106, no. 16, p. 165005, Apr. 2011.

[16] C. Paoloni *et al.*, "THz backward-wave oscillators for plasma diagnostic in nuclear fusion," in *Proc. IEEE Int. Conf. Plasma Sci. (ICOPS)*, May 2015, p. 1.

[17] Y.-M. Shin, L. R. Barnett, and N. C. Luhmann, Jr., "Strongly confined plasmonic wave propagation through an ultrawideband staggered double grating waveguide," *Appl. Phys. Lett.*, vol. 93, no. 22, p. 221504, 2008.

[18] M. Mineo and C. Paoloni, "Double-corrugated rectangular waveguide slow-wave structure for terahertz vacuum devices," *IEEE Trans. Electron Devices*, vol. 57, no. 11, pp. 3169–3175, Nov. 2010.

[19] CST AG, Darmstadt, Germany. *CST Studio Suite*. [Online]. Available: http://www.cst.com

[20] B. Goplen, L. Ludeking, D. Smith, and G. Warren, "User-configurable MAGIC for electromagnetic PIC calculations," *Comput. Phys. Commun.*, vol. 87, nos. 1–2, pp. 54–86, May 1995.

AQ:7

Claudio Paoloni (M'86–SM'11) received the Laurea degree in electronics engineering from the University of Rome Sapienza, Rome, Italy, in 1984.

He has been a Professor of Electronics with the Department of Engineering, Lancaster University, Lancaster, U.K., since 2012, where he is currently the Head of the Engineering Department.

Diana Gamzina received the B.S. degrees in mechanical engineering and materials science and the M.S. degree in mechanical engineering, in 2008 and 2012, respectively, and the Ph.D. degree with a focus on the thermomechanical design and analysis of high power and high frequency vacuum electronics.

She has been a Staff Member with the Millimeter-Wave Research Group, University of California at Davis, Davis, CA, USA, since 2008.

AQ:8

Logan Himes received the B.S. degrees in biotechnology and applied microbiology from the University of California at Davis (UC Davis), Davis, CA, USA, in 2010.

He has been an Associate Development Engineer with the Millimeter-Wave Research Group, UC Davis, since 2010, where he has been involved in the development of precision and high performance micro and nanomachining and manufacturing strategies and techniques for the production of high frequency vacuum electronics.

Branko Popovic is currently pursuing the Ph.D. degree with the Department of Electrical and Computer Engineering, University of California at Davis (UC Davis), Davis, CA, USA.

He is a member of the Millimeter-Wave Research Center with UC Davis. His current research interests include millimeter-wave vacuum electronics, under the guidance of Prof. N. Luhmann, with a main focus on the design of vacuum electronic devices using electromagnetic and particle in cell codes, and laboratory testing of these devices and related components.

AQ:9

Robert Barchfeld is currently pursuing the Ph.D. degree with the Department of Applied Science, University of California at Davis, Davis, CA, USA.

His current research interests include plasma physics and fusion technology under the guidance of Prof. N. Luhmann, the design, construction, and implementation of plasma diagnostic instruments, vacuum electronics, microfabrication, and related millimeter-wave technologies.

AQ:10

Lingna Yue, photograph and biography not available at the time of publication.

Yuan Zheng, photograph and biography not available at the time of publication.

Xiaopin Tang, photograph and biography not available at the time of publication.

Ye Tang, photograph and biography not available at the time of publication.

Pan Pan received the B.S. degree in engineering from Tsinghua University, Beijing, China, in 2010, and the M.S. degree in physical electronics from the Beijing Vacuum Electronics Research Institute (BVERI), Beijing, in 2015.

He joined BVERI in 2010, as an Assistant Engineer, where he is involved in developing W-band TWTs.

Hanyan Li, photograph and biography not available at the time of publication.

Rosa Letizia (M'13) received the Ph.D. degree in computational photonics from the University of Leeds, Leeds, U.K., in 2009.

She has been a Lecturer with the Engineering of Microwave, Terahertz and Light Group, Engineering Department, Lancaster University, Lancaster, U.K., and the Cockcroft Institute, Warrington, U.K., since 2011.

Mauro Mineo received the Ph.D. degree in telecommunication and microelectronic engineering from the University of Rome Tor Vergata, Rome, Italy.

He was a Research Associate with the Engineering Department, Lancaster University, Lancaster, U.K., from 2012 to 2015. He has been with e2v Technologies Ltd., Chelmsford, U.K., since 2015, as an RF/Microwave Modeling Engineer.

Jinjun Feng (M'94–SM'06) is currently the Vice Chief-Engineer and the Head of the Vacuum Electronics National Laboratory with the Beijing Vacuum Electronic Research Institute, Beijing, China. He has authored or co-authored one book, one book chapter, and over 200 papers in domestic and overseas conference proceedings and scientific journals.

Mr. Feng has been a fellow of the Chinese Institute of Electronics since 2013 and a member of the IEEE Electron Devices Society of the Vacuum Electronic Technical Committee since 2010. He was the Chair of the IEEE Electron Devices Society Beijing Chapter from 2011 to 2012, and he has been the Chair of the IEEE Beijing Section since 2014.

Neville C. Luhmann, Jr. (F'–) received the Ph.D. degree from the University of Maryland at College Park, College Park, MD, USA, in 1972. AQ:11

He is currently a Distinguished Professor with the Department of Electrical and Computer Engineering, University of California at Davis, Davis, CA, USA, where he is also a Co-Director of the Millimeter-Wave Research Center.

AUTHOR QUERIES

AUTHOR PLEASE ANSWER ALL QUERIES

PLEASE NOTE: Please note that we cannot accept new source files as corrections for your paper. If possible, please annotate the PDF proof we have sent you with your corrections and upload it via the Author Gateway. Alternatively, you may send us your corrections in list format. You may also upload revised graphics via the Author Gateway.

AQ:1 = Please confirm whether the edits made in the financial section are OK.
AQ:2 = Please confirm the postal codes for "Lancaster University, University of Electronic Science and Technology of China, Beijing Vacuum Electronic Research Institute, e2v Technologies Ltd."
AQ:3 = Please confirm the organization name "Beijing Vacuum Electronic Research Institute." And company name "e2v Technologies Ltd."
AQ:4 = Please provide the expansions for the acronyms "MEMS, CNC, MPCVD, and DTL."
AQ:5 = Please provide the captions for "Tables I and II."
AQ:6 = In Fig. 4, text is too small and difficult to read. Please provide clearer assembled image with more legible text.
AQ:7 = Please confirm the title and also provide the accessed date for ref. [19].
AQ:8 = Please provide the university name for the degrees received for the author "Diana Gamzina."
AQ:9 = Please confirm whether the edits made in the sentence "His current research … related components." are OK.
AQ:10 = Please confirm whether the edits made in the sentence "His current research … millimeter-wave technologies." are OK.
AQ:11 = Please provide the membership year for the author "Neville C. Luhmann."

Aq:1 mauro.mineo@e2v.com
AQ2: Confirmed
AQ3 Confirmed
AQ4: MEMS Micro-Electro-Mechanical Systems
CNC computer numerical control
MPCVD microwave plasma chemical vapor deposition
DTL has no expansion : iit s the name of the company
AQ5: Caption Table I
"SWS Dimensions"
Caption Table II
"BWO Specifications"
AQ6 new figures included. Please replace 4a,b,c,d
AQ7 confirmed 2010
AQ8:Confirmed, University of California Davis
AQ9 ok
AQ10: ok
AQ:11(SM'95–F'02)